Smectic Liquid-Crystalline Phases of Quaternary Group VA (Especially Phosphonium) Salts with Three Equivalent Long *n*-Alkyl Chains. How Do Layered Assemblies Form in Liquid-Crystalline and Crystalline Phases?

David J. Abdallah,[†] Allan Robertson,[‡] Hsiu-Fu Hsu,[§] and Richard G. Weiss*,[†]

Contribution from the Department of Chemistry, Georgetown University, Washington, D.C. 20057-1227, Cytec Industries Inc., Niagara Falls, Ontario, Canada L2E 6T4, and Department of Chemistry and Biochemistry, Massachusetts Institute of Technology, Cambridge, Massachusetts 02139

Received November 18, 1999

Abstract: The neat phase behavior of 28 phosphonium salts (**nPmA**), each with three equivalent long *n*-alkyl chains containing **m** carbon atoms and one shorter chain containing **n** carbon atoms or a benzyl group, have been examined. Eighteen form a liquid-crystalline smectic A_2 (SmA_2) phase, where the lipophilic chains assemble in bilayers that sandwich an "ionic plane" consisting of an array of anions and positively charged phosphorus atoms. Several analogous ammonium salts are examined as well. These are the first structures reported for liquid-crystalline amphiphiles containing three equivalent long *n*-alkyl chains and a single atom headgroup. In addition, the **nPmA** demonstrate how the steric interactions of lipophilic chains and electrostatic interactions among the ionic parts must be balanced in layered assemblies when the cross-sectional area of the chains is much larger than that of the headgroups. A model is proposed to explain the dependence of layer thicknesses in the liquid-crystalline phases of the **nPmA** on **m**, **n**, and the size of the anion. A comparison is made of the packing modes among analogous Group VA salts (N.B., N or P) with 1−4 long *n*-alkyl chains (and the remainder as methyl groups) in their neat crystalline and liquid-crystalline phases.

Introduction

The molecular assemblies of quaternary salts comprised of a Group VA cationic headgroup (N.B., N, or P) and *one*[1] or *two*[2] long *n*-alkyl chains[3] have been studied extensively. Many form either smectic phases when neat or other assemblies, such as micelles, when mixed with water.[4] Recently, we reported the packing arrangements for crystalline phases of several Group VA salts containing *four* equivalent long *n*-alkyl chains; none is liquid-crystalline.[5] To complete the series, we examine here the anisotropic phases of 28 phosphonium salts (**nPmA**) with *three* long equivalent *n*-alkyl chains (containing **m** = 10, 14, or 18 carbon atoms each), one shorter chain with **n** = 0−5 carbon atoms or a benzyl group (**Bz**), and anions (**A**) of various types and sizes (Table 1). Their properties and those of some corresponding ammonium salts (**nNmA**) are compared.[6] No **nYmA** salts with "simple" **A** groups and **Y** = As, Sb, or Bi were found in the Cambridge Structural Database or in Beilstein. Because the sum of the cross-sectional areas of the three long chains is much larger than that of an N or P centered headgroup, assemblies somewhat like those of the tetra-*n*-alkyl salts, in which the ionic parts are arranged in planes that bisect pairs of chains on each molecule,[5] were anticipated. Instead, 18 of the **nPmA** and the corresponding **nNmA** investigated organize into smectic A_2 (SmA_2) phases, (i.e., *bi*layered assemblies that are also liquid-crystalline[7]).

Explanations advanced to reconcile the data complement the well-founded models of Israelachvilli and others for predicting the packing arrangements of surfactant molecules with one or two long chains, especially in aqueous media.[8] The conclusions derived from this work provide the first comprehensive picture of the consequences of progressively increasing the ratio between the cross-sectional areas of the chains and the areas of their headgroups in *neat phases* of these structurally simple amphiphiles. They demonstrate that, unlike in lyotropic phases, the natures of the anions (as well as the size of the **n** group on N or P) play a *central* role in the overall packing arrangements of the cationic parts. Most importantly, they answer a very

[†] Georgetown University.
[‡] Cytec Industries Inc.
[§] Massachusetts Institute of Technology.

(1) (a) Gault, J. D.; Gallardo, H. A.; Muller, H. J. *Mol. Cryst. Liq. Cryst.* **1985**, *130*, 163. (b) Busico, V.; Cernicchiaro, P.; Corradini, P.; Vacatello, M. *J. Phys. Chem.* **1983**, *87*, 1631. (c) Busico, V.; Corradini, P.; Vacatello, M. *J. Phys. Chem.* **1982**, *86*, 1033. (d) Margomenou-Leonidopoulou, G.; Malliaris, A.; Paleos, C. M. *Thermochim. Acta* **1985**, *85*, 147.

(2) (a) Kanazawa, A.; Tsutsumi, O.; Ikeda, T.; Nagase, Y. *J. Am. Chem. Soc.* **1997**, *119*, 7670. (b) Alami, E.; Levy, H.; Zana, R.; Weber, P.; Skoulios, A. *Liq. Cryst.* **1993**, *13*, 201.

(3) In this work, the arbitrary definition of a "long chain" is ≥10 carbon atoms.

(4) (a) Margomenou-Leonidopoulou, G. *J. Therm. Anal.* **1994**, *42*, 1041. (b) Margomenou-Leonidopoulou, G. *ICTAC News* **1993**, *26*, 24. (c) Tschierske, C. *J. Mater. Chem.* **1998**, *8*, 1485. (d) Tschierske, C. *Prog. Polym. Sci.* **1996**, *21*, 775.

(5) Abdallah, D. J.; Bachman, R. E.; Perlstein, J.; Weiss, R. G. *J. Phys. Chem. B* **1999**, *103*, 9269.

(6) Lu, L.; Sharma, N.; Nagana Gowda, G. A.; Khetrapal, C. L.; Weiss, R. G. *Liq. Cryst.* **1997**, *22*, 23.

(7) A bilayer smectic A phase is denoted as SmA_2. Demus, D.; Goodby, J.; Gray, G. W.; Spiess, H.-W.; Vill, V. *Handbook of Liquid Crystals, High Molecular Weight Liquid Crystals*; Wiley-VCH: New York, 1998; Vol. 3, p 312.

(8) (a) Israelachvili, J. N. *Intermolecular and Surface Forces*, 2nd ed.; Academic Press: London, 1992; Chapter 17. (b) Israelachvili, J. N.; Mitchell, D. J.; Ninham, B. W. *J. Chem. Soc., Faraday Trans. 2* **1976**, *272*, 1525.

10.1021/ja994055g CCC: $19.00
Published on Web 03/16/2000

Table 1. Structures and Properties of **mPmA** Salts

$H(CH_2)_nP[(CH_2)_mH]_3^+A^-$ (**nPmA**)			transition temp (°C)[a]		elemental analysis					
					calcd for			found		
n	**m**	A	K−SmA_2	SmA_2−I or K−I	C	H	X[b]	C	H	X
1	10	BF_4	32.5	49.3	66.89	11.95		66.97	12.01	
1	10	ClO_4		40.3−43.6	65.41	11.96		65.53	11.75	
1	10	PF_6		55.0−56.1	60.58	10.82		60.72	10.90	
1	14	Cl		105.0−105.5						
1	14	Br	103.5	112.4	71.93	12.63	11.13 (Br)	72.05	12.74	11.03
1	14	NO3	43.4	110.4	73.76	12.96	2.00 (N)	73.84	13.01	1.97
1	14	BF_4	52.6	100.6	71.24	12.51		71.33	12.63	
1	14	ClO_4	60.9	103.2	70.02	12.30		70.12	12.33	
0	18	Br		103.1−106.7						
0	18	I	94.3	109	70.55	12.28	13.80 (I)	70.78	12.14	13.85
1	18	Cl		95.5−97.5	78.46	13.65	4.21 (Cl)	78.29	13.85	4.18
1	18	Br	99.4	106.9	74.53	12.96	9.02 (Br)	74.44	12.94	9.37
1	18	I	73.1	113.5	70.77	12.31	3.32 (I)	70.68	12.10	3.17
1	18	NO_3	69.4	107.8	76.06	13.23	1.61 (N)	75.92	13.30	1.76
1	18	BF_4	69.6	105.4	73.95	12.86		73.87	12.94	
1	18	ClO_4	75.4	107.6	72.92	12.68	3.91 (Cl)	72.84	12.77	3.92
1	18	PF_6	79.8	92.3	69.43	12.08		69.61	12.25	
1	18	EX	54.6	59.2						
2	18	Br	94.4	97.8	74.70	12.98	8.87 (Br)	74.61	13.13	9.04
2	18	I	86.8	107.6	71.00	12.34	13.40 (I)	71.25	12.12	13.17
3	18	Br		79.6−81.9						
3	18	I		86.9−88.7 (87.4)	71.21	12.37	13.20 (I)	71.41	12.34	13.12
4	18	I		86.7−88.5 (77.9)	71.42	12.40	13.01 (I)	71.24	12.29	13.21
5	18	I		82.9−84.9						
7 (Bz)[c]	18	Br	72.1	78.5						
12	18	I		83.9−85.0						
18	18	Br		92.3−94.8						
18	18	I		97.6−99.3						

[a] By optical microscopy; see ref 11. Numbers in parentheses are for monotropic I-SmA_2 transitions. See Table 2 (**1PmA**) and Tables 1 (**nP18Br**) and 2 (**nP8I**) in the Supporting Information for transition temperatures by DSC. [b] Element analyzed in parentheses. [c] **Bz** is benzyl; **EX** is ethyl xanthate.

important question implicitly unresolved by existing theories for packing of charged surfactant molecules in neat phases: *How are the neat assemblies of such molecules organized?*

In addition, these salts have many potential applications. For instance, they are a new class of oriented "green" ionic solvents[9] in which reacting solute molecules may undergo selective reactions due to ordering by the medium.[10] Applications demonstrating their utility will be presented elsewhere.

Experimental Section

Cations were characterized by ^1H, ^{31}P, and ^{19}F NMR spectroscopies (when appropriate) using a Varian 300 MHz spectrometer interfaced to a Sparc UNIX computer with Mercury software. Chemical shifts were referenced to internal TMS (^1H) or an external 85% H_3PO_4 (^{31}P) or CCl_3F (^{19}F) standard. Midwest Microlab, Indianapolis, IN, performed all elemental analyses reported in Table 1 except that for **1P18I** (by Desert Analytics, Tucson, AR). Spectroscopic data are reported as Supporting Information.

Examination of Phases. Thermally induced phase changes of the phosphonium salts were followed by differential scanning calorimetry (**DSC;** TA 2910 DSC cell base interfaced to a TA Thermal Analyst 3100 controller equipped with a hollowed aluminum cooling block into which dry ice was placed for subambient measurements), polarizing optical microscopy (Leitz 585 SM-LUX-POL microscope equipped with crossed polars, a Leitz 350 heating stage and an Omega HH21 Microprocessor thermometer connected to a K thermocouple), and X-ray diffractometry (Inel CPS 120 diffractometer, Cu_α radiation, and a home-built sample thermostating unit).

Samples for optical microscopy were either sandwiched between glass slides or placed in cells constructed of glass slides separated by 25 μm Mylar strips and held together by epoxy glue. Liquids (above the melting temperature, T_{K-SmA_2}[11]) flowed into the heated cells by capillary action. Once the cells had cooled to below T_{K-SmA_2}, the edges were sealed with epoxy to prohibit liquid flow. Samples (3−5 mg) were placed in open aluminum pans for **DSC** analyses. A steady stream of nitrogen flowed through the cell. For samples examined only above ambient temperatures, the heating rate was 5 °C/min and the cooling rate was uncontrolled and depended on the difference between the sample and ambient temperatures. For samples examined below ambient temperatures (−40 to 120 °C), the heating and cooling rates were 5 °C/min. Samples for X-ray diffraction studies were sealed in 1 mm capillaries (Charles Supper Company, Natick, MA).

Syntheses of Salts. Two typical synthetic procedures are provided below. Detailed procedures for preparation of the other salts and associated spectroscopic and analytical information are included as Supporting Information. The general methodologies are outlined in Scheme 1. Phase transition temperatures by optical microscopy and elemental analyses are collected in Table 1.

Tridecylmethylphosphonium Ethyl Xanthate (1P10EX). In a sealed glovebag purged with nitrogen, 25 mL (50 mmol) of a 2.0 M anhyd bromomethane in *tert*-butyl methyl ether, 21.22 g (47 mmol) of **TDP**, and 40 mL of chloroform were stirred in an ice-bath that was allowed to melt slowly. Stirring was continued for 1 day, 8.0 g (50 mmol) of potassium ethyl xanthate was added, and the yellow solution was stirred for an additional day. The mixture was filtered and the volume of the filtrate was adjusted to 100 mL with $CHCl_3$ to form a 0.47 M solution, assuming complete conversion of **TDP** to **10P1EX**. This solution was used to synthesize other **1P10A** salts.

Tridecylmethylphosphonium Tetraflouroborate ($1P10BF_4$). The procedure described for **$1P10BF_4$** was employed to prepare the other

(9) (a) Seddon, K. R. *J. Chem. Technol. Biotechnol.* **1997**, *68*, 351. (b) Ming Lee, K.; Kuan Lee, C.; Lin, I. J. B. *J. Chem. Soc., Chem. Commun.* **1997**, 899. (c) Gordon, C. M.; Holbrey, J. D.; Kennedy, A. R.; Seddon, K. R. *J. Mater. Chem.* **1998**, *8*, 2627.

(10) Weiss, R. G. *Tetrahedron* **1988**, *44*, 3413.

(11) Acronyms for phase transitions are as follows: K−K ⟹ solid−solid; K−SmA_2 ⟹ solid-smectic A_2; K−I ⟹ solid-isotropic; SmA_2−I ⟹ smectic A_2-isotropic.

Scheme 1. Structures of Ammonium Salts and Synthetic Pathways to Phosphonium Salts Discussed in the Text

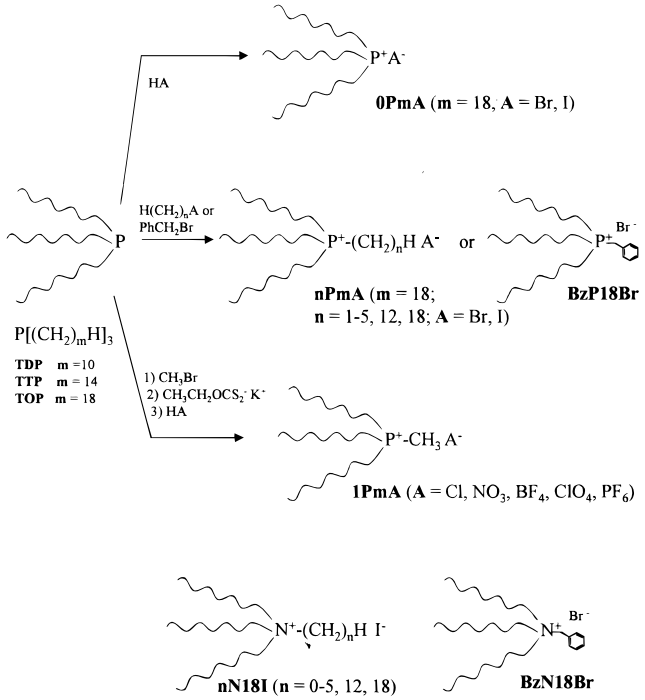

1P10A. **1P10EX** (25 mL, 11.67 mmol, 0.47 M) and 2 mL (48%, 15 mmol) of HBF_4 were stirred in an ice-bath that was allowed to melt slowly. After 1 day the organic layer was washed with HPLC grade water (3 × 25 mL). The organic layer was concentrated to a yellow oil that was crystallized (3×) from acetone at −77 °C and filtered on a Buchner funnel packed in dry ice, affording 2.96 g (46%) of a white solid at −77 °C and a transparent deformable solid (after drying in a vacuum desiccator beside P_2O_5) at room temperature: T_{K-SmA_2} 32.5 °C, T_{SmA^2-I} 49.3 °C. ^{1}H NMR ($CDCl_3$) δ 2.15 (m, 6H), 1.83 (d, J_{P-CH_3} 13.5 Hz, 3H), 1.48 (m, 12H), 1.25 (m, 36H), 0.88 (t, *J* 6.6 Hz, 9H) ppm. ^{31}P NMR ($CDCl_3$) δ 32.2 ppm. ^{19}F NMR ($CDCl_3$) δ −151.6 (^{10}B**F$_4$**), −151.7 (^{11}B**F$_4$**) ppm. See Table 1 for elemental analysis.

Results

In a preliminary report, we described the syntheses and mesophase properties of a series of corresponding alkyltrioctadecylammonium halides (**nN18A**, where **A** is for the most part iodide).[6] The **nPmA** are much more stable to heat and exhibit wider liquid-crystalline temperature ranges and lower onset temperatures. The mesophases of the **mPnA** and **mNnA** salts[12] are identified as smectic A_2 (SmA_2)[7] from the onset, although justification will be developed throughout the text.[13] In a SmA_2 phase, the constituent molecules are in repeating bilayer units. The directors of the molecules are orthogonal to the layer planes, on average, but there is no additional intermolecular ordering within the plane.

Synthetic Procedures. The structures of the **nPmA** used in this study are shown in Table 1. The syntheses of the ammonium salts have been described elsewhere.[6] Salts of **nPmA** (**A** = Br, I) were synthesized in one step by mixing a trialkylphosphine and an appropriate alkyl halide or acid under an oxygen-free atmosphere (Scheme 1). Iodide salts were synthesized in the dark since their solutions became yellow when exposed to light. Fortunately, impurities from the phosphine reagents, including those resulting from phosphines with branched chains, could be removed conveniently by repeated recrystallization of crude products. The impurities are detectable in NMR spectra of the initially isolated salts but not after recrystallizations.

Anions were exchanged by stirring a colorless chloroform solution of **1PmBr** over solid (yellow) potassium ethyl xanthate.[14] For best results, the reagent should be prepared fresh rather than using commercial xanthate. As indicated by the increased intensity of the yellow color in the chloroform solution over time, ethyl xanthate replaced bromide, forming **1PmEX** (Scheme 1). Addition of a protic acid decomposes the ethyl xanthate anion of **1PmEX** to carbon disulfide and ethanol, leaving $\mathbf{A}^-$ to combine with $\mathbf{1Pm}^+$. In this way, a variety of **1PmA** was prepared in good chemical yields and in high purities.[15,16] As indicated by **DSC**, the phosphonium salts could be stored in the air and heated repeatedly to their clearing temperatures without decomposition. The corresponding ammonium salts are unstable near their clearing temperatures.[6]

Thermodynamic Properties and Phase Transition Temperatures. Transition temperatures and heats and entropies of transitions for **nP18Br** and **nP18I** from **DSC** measurements are given in Tables 1 and 2 in the Supporting Information. **DSC** derived data for the **1PmA** are given in Table 2. A typical thermogram of **1P14ClO$_4$** is displayed in Figure 1 and can be reproduced in subsequent scans. Thermograms from the first heating of the solvent-crystallized morph of most salts contain an additional low ΔH solid−solid[11] transition that is not present in the second heating scan. The reproducibility of the second and subsequent heating thermograms and all cooling thermograms provide compelling evidence for the aforementioned thermal stability of the salts. They also demonstrate that the morphs obtained by solvent recrystallization and melt cooling are not always the same.

Although enthalpies of the solid → SmA_2 transitions of the enantiotropic (***e***) liquid-crystalline salts (**0P18I, 1P18A** (**A** = Br**,** I**,** NO_3**,** BF_4**,** ClO_4**,** PF_6), **2P18A** (**A** = Br**,** I), and **BzP18Br**) vary over a wide range, most are near 80 kJ/mol, and those with lower values have an additional solid−solid transition close in temperature. The enthalpies of all of the SmA_2 → isotropic transitions are 2.7−4.3 kJ/mol. ΔH values for the isotropic → (monotropic, ***m***) SmA_2 transitions of **3P18I** and **4P18I** are similar to those found for the enantiotropic ones. The **4P18I** suffers more hysteresis than **3P18I**.

Data in Figure 2 provide insights into the relationship between structures and liquid-crystalline properties (especially transition temperatures) of the tri-*n*-octadecyl salts, **nP18Br, nP18I**, and

(12) Unfortunately, none of the salts, except **BzN18Br**,[12a] has provided single crystals suitable for X-ray structural analysis thus far. Efforts to produce others continue. (a) Abdallah, D. J.; Lu, L.; Cocker, T. M.; Bachman, R. E.; Weiss, R. G. *Liq. Cryst.* In press.

(13) Previously,[6] we assigned the liquid-crystalline phase of methyltri-*n*-octadecylammonium iodide as nematic based on its ability to be aligned by a strong magnetic field. That assignment is incorrect for the neat material. The phase designations of the ammonium salts are based on their optical micrographs and XRD patterns (which are like those of the **nPmA** salts). They will not be discussed here except in comparative terms.

(14) A modification of the literature procedure: Sepulveda, L.; Cabrera, W.; Gamboa, C.; Meyer, M. *J. Colloid Interface Sci.* **1987**, *117*, 460.

(15) The liquid-crystalline properties of **1PmA** with organic anions will be reported elsewhere. Such salts were formed by addition of the corresponding organic acids to**1PmEX**. After crystallization from acetonitrile, they were hydrates (^{1}H NMR). Of the **nPmA** with organic anions synthesized thus far, only **1P18EX** and methyltrioctadecylphosphonium benzoate are liquid-crystalline.

(16) Attempts to synthesize methyltri-*n*-octadecylphosphonium fluoride using the anion-exchange procedure,[14] but in polyethylene bottles, led to a salt in which the **1P18** cation could be identified (by ^{1}H and ^{31}P NMR), but no ^{19}F NMR signal was found. In the DSC thermograms, an endothermic melting transition at 76.8 °C was followed by a large exotherm at 78 °C, and each subsequent scan was different from the previous one. Because this behavior probably corresponds to decomposition, no further studies were performed on this material.

Table 2. Transition Temperatures, Enthalpies (ΔH), and Entropies (ΔS) of **1PmA** from **DSC** Thermograms

			first cooling		second heating		
m	**A**	transition[a]	T (°C)[b]	ΔH (kJ/mol)	T (°C)	ΔH (kJ/mol)	ΔS[c] (J/mol·T(K))
18	Cl	K−K	67.1	10.1	–	–	–
			76.4	5.0	53.3	1.1	–
			80.4	48.3	71.4	4.2	–
		K−I	91.8	12.5	89	101.0	–
	Br	K−K	–	–	–	–	–
			70.0	66.1	82.2	62.0	183.5
		K−SmA_2	95.3	12.0	94.5	12.1[s]	32.7
		SmA_2−I	103.0	3.3	102.7	2.8[s]	8.1
	I	K−K	45	16.2	48	20.2	–
			55.7	33.8	60.4	−11.7	–
		K−SmA_2	67.6	2.8	68.7	60.6	–
		SmA_2−I	112.2	3.6	112.6	3.4	9.1
	NO_3	K−K	–	–	–	–	–
		K−SmA_2	56.2	62.6	66.3	67.0	193.9
		SmA_2−I	106.1	3.0	105.5	2.9	7.7
	BF_4	K−K	59.2	17.9	–	–	–
		K−SmA_2	64.6	48.4[s]	67.6	86.0[s]	–
		SmA_2−I	104.1	3.5	104.5	3.3	9.0
	ClO_4	K−K	–	–	–	–	–
		K−SmA_2	67.2	82.9	72.8	83.8	242.9
		SmA_2−I	105.2	3.3	105.3	3.0	8.3
	PF_6	K−K	73.4	87.7	–	–	–
		K−SmA_2	81.1	5.6	79.6	92.0	–
		SmA_2−I	96	2.9	96	3.1	8.2
	EX	K−SmA_2	49.1	92.7	52.5	95.2	290.1
		SmA_2−I	59.5	2.8	59.4	3.3	9.2
14	Cl	K−K	50.6	39.5	64.1	44.2	126.7
		K−I	92	7.7	83.8	9.7	24.1
	Br	K−K	64.3	28.2	57.5	41.6	–
		K−SmA_2	98.3	9.1	98.2	9.7	25.3
		SmA_2−I	108.0	3.9	108.6	3.7	10.1
	NO_3	K−K	–	–	22.3	−18.4	–
			14.1	39.2	37.1	44.7	–
		K−SmA_2	54.7	1.6	48.8	1.3	4.5
		SmA_2−I	107.4	3.6	106.8	3.6	9.5
	BF4	K−K	28.1	30.6	37.6	35.1	107.3
		K−SmA_2	51.4	3.6	53.3	3.8	11.5
		SmA_2−I	96	3.1	96.9	3.3	8.6
	ClO_4	K−K	31.5	59.5	47.6	57.0	186.4
		K−SmA_2	55.5	3.9	57.6	3.6	11.4
		SmA_2−I	96.3	3.2	97.7	3.3	8.9
10	BF_4	K−K	−30.6	15.1	−27.2	−15.7	–
			–	–	7.0	40.0	–
		K−SmA_2	27.8	2.1	31.0	2.2	7.1
		SmA_2−I	46.1	3.0	48.5	2.9	9.3
	ClO_4	K−K	–	–	−29.0	−32.3	–
			–	–	12.9	37.4	–
		K−I	35.0	4.7	38.7	4.7	15.2
	PF_6	K−K	−29.4	5.1	−18.4	6.1	–
			–	–	30.2	16.4	–
		K−I	48.4	7.3	51.0	7.1	22.3

[a] Reference 11. [b] Peak onset. [c] ΔS calculated from the averaged ΔH and T based on the first cooling and second heating thermograms. –, no transition was observed; s, shoulder peak; o, two overlapping peaks.

nN18I.[6] The **nP18I** consistently have lower $T_{K\rightarrow SmA}$[2][11] and broader mesophase ranges than the corresponding **nN18I**. When **nP18A** anions are bromide, the mesophases either exhibit much narrower ranges or are not present. Entropies of transitions (ΔS) for reversible transitions were calculated as well using ΔH values from the first cooling and second heating **DSC** curves and their onset temperatures. The $\Delta S_{SmA_2\rightarrow I}$ trends for these salts indicate that **n** (i.e., the size of the varied alkyl group) has a large influence on the order within an SmA_2 phase. As with the other salts, **BzP18Br** is thermally stable to above its (***e***) SmA_2-isotropic clearing temperature, but **BzN18Br** is not.[6] The **1P18A** with large anions (i.e., nitrate, perchlorate, tetrafluoroborate, and hexafluorophosphate) have similar mesophase ranges and T_{SmA_2-I} values that differ from those of the bromide salt. Since liquid-crystalline ranges are largest when the fourth substituent is methyl (**n** = 1), we will focus primarily on salts with **1Pm** cations.

Decreasing **m** from 18 to 14 in **1PmA** results in increasingly wider liquid-crystalline ranges as a result of lower T_{K-SmA_2} values (Figure 3). The lower temperature solid−SmA_2 transition corresponds to chain melting whereas the higher temperature SmA_2−isotropic transitions correspond to loss of the stronger interactions within an ionic plane.[17] However, this trend does not extend to **m** = 10 salts (Figure 3); there, entropic disorder caused by chain melting (and subsequent disruption of the ionic planes via molecular tumbling) and greater electrostatic interactions of neighboring ionic layers appear to be more important than attractive van der Waals forces. Only **1P10A** with **A** = BF_4 was a (enantiotropic) liquid crystal (Table 2), and that over

(17) Paleos, C. M. *Mol. Cryst. Liq. Cryst.* **1994**, *243*, 159.

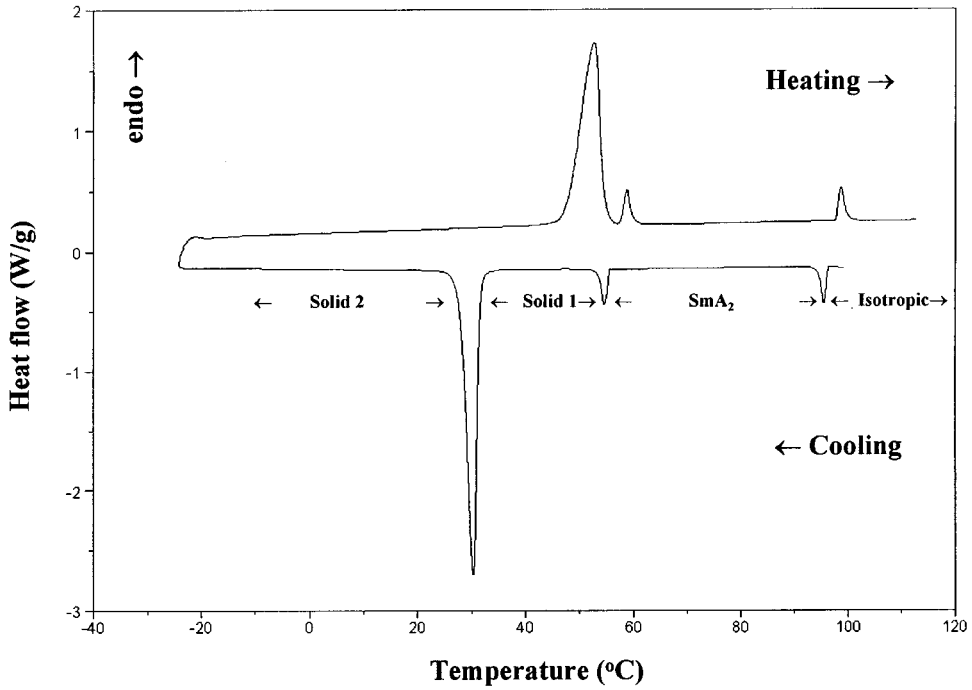

Figure 1. DSC thermogram of **1P14ClO$_4$** (see Experimental Section for details). The sample was cooled from the isotropic melt and then heated at a rate of 5 °C/min.

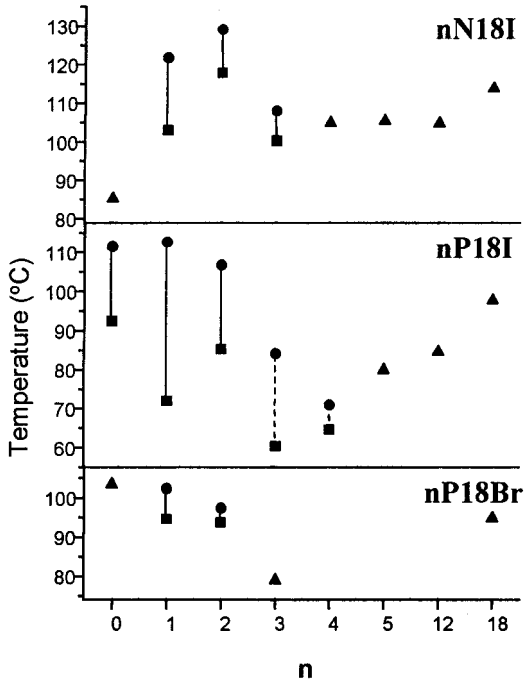

Figure 2. Phase transition temperatures from the onset of peaks in **DSC** thermograms of **nN18I** (ref 6) and **nP18A**. Transition temperatures are for melting (▲, T_m), solid-SmA$_2$ (■, T_{K-SmA_2}), and SmA$_2$-isotropic (●, T_{SmA_2-I}) transitions. Solid lines indicate temperature ranges of enantiotropic phases from first heating and dotted lines indicate temperature ranges of monotropic phases from first cooling.

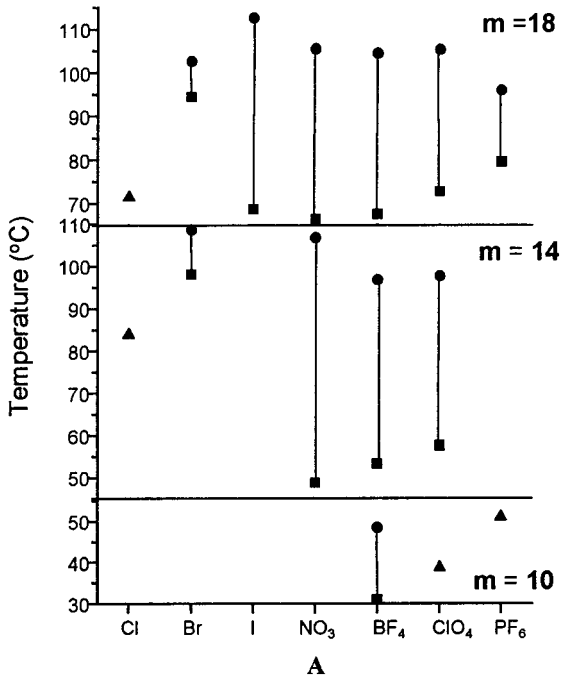

Figure 3. Phase transition temperatures from the onset of peaks in **DSC** thermograms of **1PmA**. Transition temperatures are for melting (▲, T_m), solid-SmA$_2$ (■, T_{K-SmA_2}), and SmA$_2$-isotropic (●, T_{SmA_2-I}) transitions. Solid lines indicate temperature ranges of enantiotropic phases from second heating.

a narrow temperature range. Orientational order is concomitantly lost upon chain melting for **1P10ClO$_4$** and **1P10PF$_6$**. Similarly, $\Delta H_{K\rightarrow I}$ of the nonmesomorphic **1P18Cl** (or **1P14Cl**) is 3−4× larger than $\Delta H_{SmA_2\rightarrow I}$ of **1P18Br** and **1P18I** despite the clearing temperatures for the**1P18A** being in the following order: Cl < Br < I.

If the solid → SmA$_2$ transitions are due exclusively to melting of alkyl chains within lamellae[17] and the heat component due to the volume changes that accompany the chain melting transitions[18] of all **1P18A** salts are similar, the difference between $3\Delta H_{BT\rightarrow I}$, the heat of melting of crystalline lamellae of *n*-alkanes of length **m**, and $\Delta H_{K\rightarrow SmA_2}$ can be related to the degree of packing disorder that is innate to chains of crystalline

(18) A part of the enthalpy for any first-order phase transition is due to volume differences between the initial and final phase. For a liquid-crystalline example, see: Price, F. P.; Wendorff, J. H. *J. Phys. Chem.* **1971**, *75*, 2839.

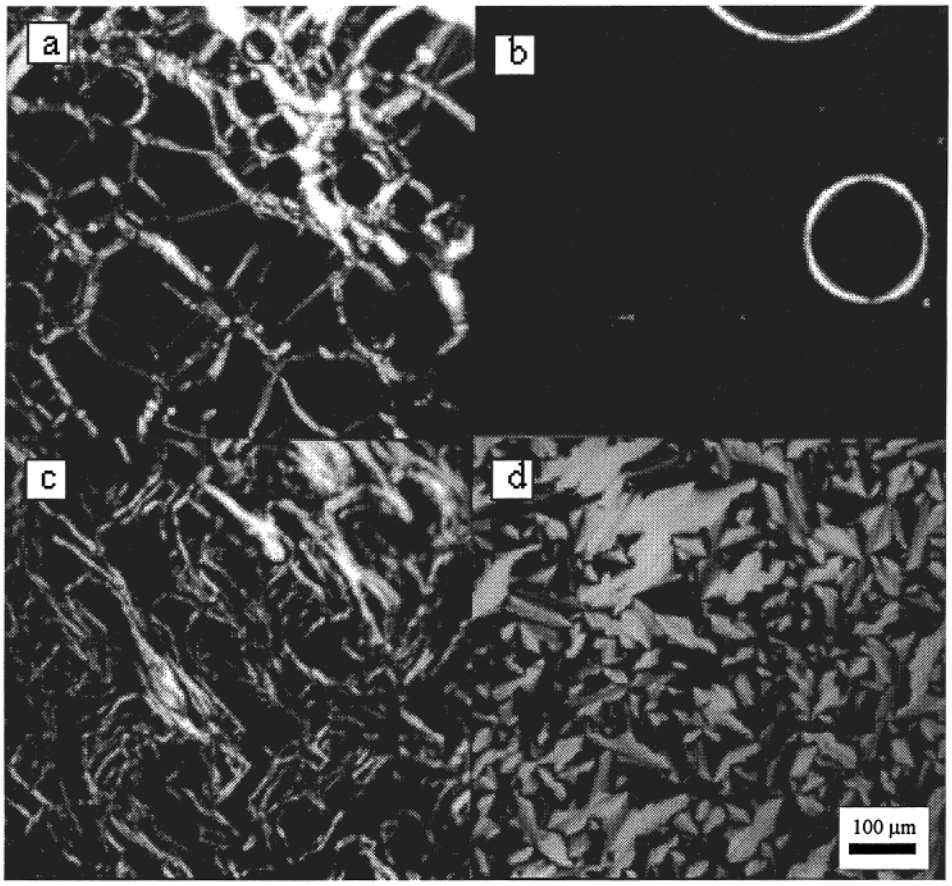

Figure 4. Optical micrographs of **1P18I** between crossed-polars at (a) 78.3 °C (first heating), (b) 74.8 °C (upon cooling), and (c) 77.0 °C (after application of lateral stress). (d) was recorded at 112 °C in a 25 μm thick cell (see text). The distance bar applies to the four micrographs.

salts and the consequent inefficient *inter*molecular van der Waals interactions. On this basis, even the chains of the salt with the largest $\Delta H_{K\rightarrow SmA_2}$ in Table 2, **1P18BF$_4$**, cannot be completely extended and parallel (as they are in crystalline *n*-octadecane[19]); their heat of melting is much less than thrice $\Delta H_{BT\rightarrow I}$ (62 kJ/mol), the enthalpy for melting crystalline *n*-octadecane.[20] In fact, all of the $\Delta H_{K\rightarrow SmA_2}$ for the **1P18A** salts are near $\Delta H_{min} = 94$ kJ/mol, the *minimum* heat necessary to melt three octadecyl chains.[21] In other work, we have shown that some gauche bends are present along chains in the crystalline phases of the tetra-*n*-alkyl Group VA salts, including **18P18I** and **12N12Br**.[5]

$\Delta H_{K\rightarrow SmA_2}$ values of the **1P18A** and the enthalpies for melting the highest temperature solid phases of analogous salts with *two* or *four* *n*-octadecyl chains can also be compared. The average heat *per octadecyl chain* from **1P18A** (**A** = NO_3 and ClO_4) and dimethyldioctadecylphosphonium chloride[2a] are almost the same, 26−29 kJ/mol-chain. The *per chain* heat for the solid → isotropic transition of **18P18I**[5] (Table 2) is somewhat larger, ca. 39 kJ/(mol·chain), because it incorporates the additional heat of headgroup melting.

Optical Microscopy. As viewed between crossed polars, liquid-crystalline **nPmA** samples cooled from the isotropic phase between glass slides are completely black (i.e., uniform homeotropic phases; Figure 4b). Samples heated initially from the solid (Figure 4a) or dislocated by lateral stress (applied to one slide) contain oily streaks (Figure 4c). Focal-conic fan textures, a common feature of smectic A phases,[22] appear when samples are cooled from the isotropic phase in 25 μm thick cells (Figure 4d).

A highly birefringent, deformable phase appears upon cooling **1P14Cl** or **1P18Cl** from its isotropic melt. Neither flows as do the liquid-crystalline materials.

X-ray Diffraction (XRD). Typically, the XRD patterns of the salts in their liquid-crystalline phases (Figure 5b) consist of a very broad, high-angle peak near $2\theta = 19.3°$ corresponding to the *intra*lamellar spacings (*D*), and at least one narrow low-angle peak in the range $2\theta = 2.5-3.1°$ corresponding to the lamellar thicknesses (*d*). The similarity between the packing arrangements of liquid-crystalline phases of **nPmA** and **nNmA** salts is exemplified by XRD patterns of **1P18I** and **1N18I** (Figure 1, Supporting Information). In several cases, higher order diffractions of the low-angle peak could be detected. Both *D* and *d* (Table 3) were calculated using Braggs law;[23] $D \cong 4.6$ Å for all of the liquid crystals. The diffractograms of **1P14Cl** and **1P18Cl** in their highly birefringent, deformable phases consist

(19) (a) Nyburg, S. C.; Gerson, A. R. *Acta Crystallogr.* **1992**, *B48*, 103 and references therein. (b) Valiyaveettil, S.; Enkelmann, V.; Mullen, K. *J. Chem. Soc., Chem. Commun.* **1994**, *18*, 2097. (c) Koh, L. L.; Xu, Y.; Gan, L. M.; Chew, C. H.; Lee, K. C. *Acta Crystallogr.* **1993**, *C49*, 1032.

(20) Broadhurst, M. G. *J. Res. Natl. Bur. Stds.* **1962**, 66A, 241.

(21) ΔH_{min} can be calculated by assuming a "crystal" chain of *n*-octadecane in which all of the C−C bonds are in gauche conformations and using 2.1 kJ/mol for the enthalpy release of a *gauche* → *transoid* bend.[21a,b] Melting consists of an *all-gauche* to *all-transoid* conformational change. Then, $\Delta H_{min} = 2.1 \times 3 \times 15 = 94$ kJ/mol is the minimum enthalpy for melting 3 octadecyl chains, each with 15 C−C bonds (excluding terminal H_3C−C linkages).[21c] (a) Sheppard, N.; Szasz, G. J. *J. Phys. Chem.* **1949**, *17*, 86. (b) Flory, P. J. *Statistical Mechanics Of Chain Molecules*; Wiley: New York, 1965; p 56. (c) Needham, G. F.; Willett, R. D.; Franzen, H. F. *J. Phys. Chem.* **1984**, *88*, 674.

(22) (a) Gray, G. W.; Goodby, J. *Smectic Liquid Crystals, Textures and Structures*; Leonord Hill: London, 1984; p 8. (b) Demus, D.; Richter, L. *Textures of Liquid Crystals*; Verlag Chemie: New York, 1978; p 61.

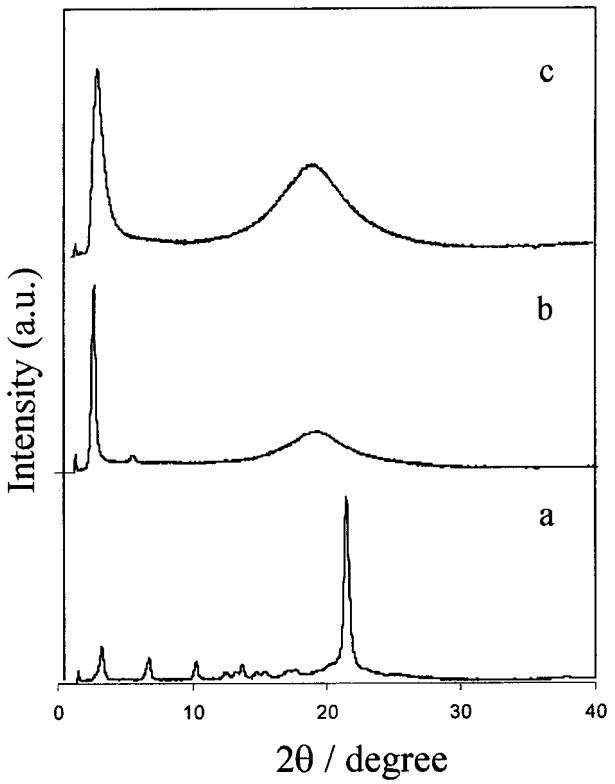

Figure 5. X-ray diffraction patterns of **1P18ClO$_4$** at (a) 60 °C (solid), (b) 90 °C (SmA_2), and (c) 110 °C (isotropic) upon first heating.

Table 3. Layer Thicknesses (*d*) from X-ray Diffraction Data, Calculated Projection Angles (see Figure 6 and text), and Cross-Sectional Areas Projected by Chains (A_{3C}) for **1PmA** Salts

m	**A**	*d* (Å)	temp (°C)[a]	ϕ (deg)	α (deg)	A_{3C} (Å^2)
18	Br	30.64	100	53	88	106
	I	32.35	80	51	84	101
		31.99	85	51	85	102
		31.64	90	52	86	103
		30.97	95	53	87	105
		30.01	100	54	89	109
		29.70	105	55	90	110
		29.11	110	55	91	112
	NO_3	34.66	80	47	79	94
	BF_4	31.80	80	52	85	102
		31.30	90	52	87	104
	ClO_4	31.30	80	52	87	104
		30.97	85	53	87	105
		30.34	90	54	88	107
		30.32	95	54	89	107
		30.01	100	54	89	109
		29.70	105	55	90	110
	PF_6	29.70	88	55	90	110
14	Br	26.95	90	49	81	97
	NO_3	27.99	75	47	79	93
	BF_4	26.46	75	50	83	99
	ClO_4	26.46	75	50	83	99
10	BF_4	20.35	43	49	81	96

[a] Temperature of collection of X-ray diffraction data.

of many sharp reflections, as expected of a solid material. They are **not** liquid-crystalline. Specifically absent was a broad, diffuse high-angle peak characteristic of melted alkyl chains.

The broadness of the *D* peak and the distance corresponding to it are consistent with van der Waals separations between disordered alkyl chains (i.e., *D* is slightly greater than the estimated cross-sectional diameter of a methylene group).[24] The

(23) Stout, G. H.; Jensen, L. H. *X-ray Structure Determination, A Practical Guide*, 2nd ed.; Wiley: New York, 1989; p 24.

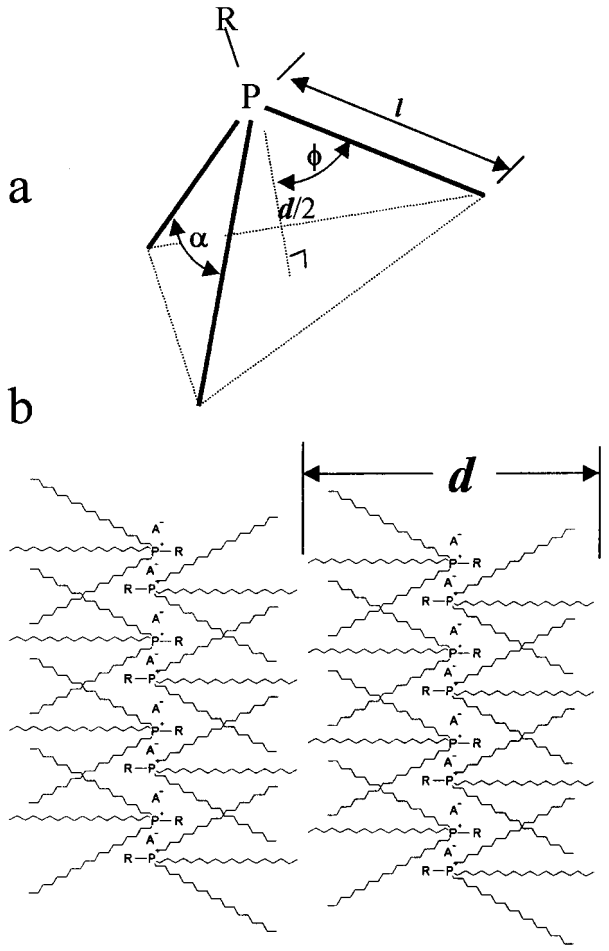

Figure 6. (a) Average conformations of cations of **nPmA**; chains represented as lines. (b) Proposed packing arrangement of **nPmA** in their SmA_2 phases. R = $H(CH_2)_n-$ or **Bz**.

values of *l* (the distance between a phosphorus nucleus and the van der Waals edge of the outermost hydrogen atom on the terminal carbon of a fully extended chain of **1Pm** cations (Figure 6a)) are 15.4, 20.5, and 25.6 Å when **m** = 10, 14, and 18, respectively. They do not correspond to the *d* spacings, nor should they if the model in Figure 6 is correct. In addition, melted alkyl chains even in a liquid-crystalline phase are not fully extended. The packing arrangement in Figure 6b is not a unique fit to the crucial data (XRD and optical microscopy) which requires the liquid-crystalline phases to be SmA_2. Our preference for this arrangement will be discussed later.

The lamellar spacings within the SmA_2 phases decrease with increasing temperature (Figure 7), apparently as a result of greater chain bending and perhaps less well-defined ionic layering (i.e., greater interpenetration). At elevated temperatures, an increase in the frequency of gauche bends shortens the distance between a cationic center and a methyl chain terminus and, thereby, decreases *d*. Surprisingly, the lamellar spacings also *decrease* when **n** ($\geq$1) of **nP18A** is *increased* (Figure 8). **0P18I**, the only salt not consistent with this trend, may behave anomalously due to either the disparity in temperatures at which the XRD patterns were measured or the presence of hydrogen-bonding interactions absent when **n** > 0. Generally, **nP18A** with longer **n** groups were examined at lower temperatures to remain within their liquid-crystalline phases. The values of *d* from **BzP18Br** and **BzN18Br** are the same within experimental error, especially when temperature is taken into account: for **BzP18Br**

(24) Skoulios, A.; Luzzati, V. *Nature* **1959**, *183*, 1310.

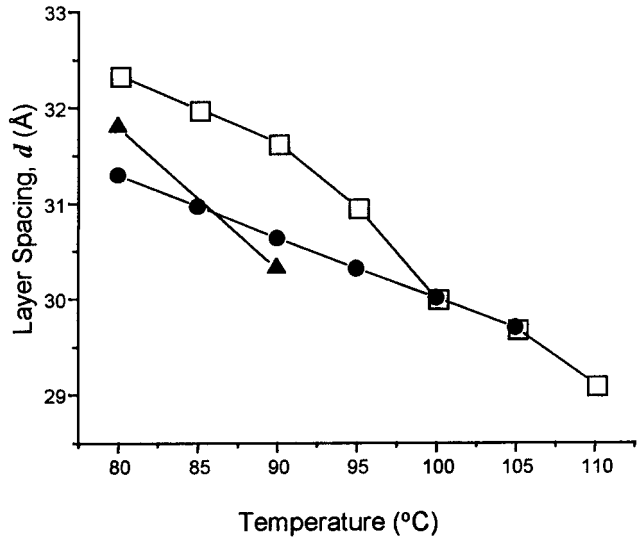

Figure 7. Temperature dependence of **1P18A** SmA_2 layer spacings. **A** = **I** (□), **ClO_4** (●), and **BF_4** (▲).

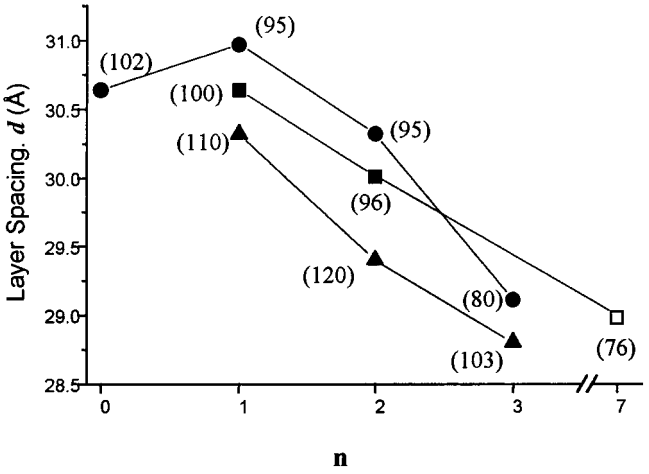

Figure 8. Dependence of SmA_2 layer spacings for various salts on **n**: **nP18I** (●), **nP18Br** (■), and **nN18I** (▲). **Bz** (□) has 7 carbon atoms. Temperatures (°C) are in parentheses.

at 76 °C, $d = 28.9$ Å; for **BzN18Br** at 90 °C, $d = 28.5$ Å. On this basis and the similarity of the high angle diffraction peaks for the two salts, their liquid-crystalline phases must be organized in the same fashion; both are SmA_2.[13]

The "isotropic" states of the salts are not completely disordered, at least at temperatures slightly above the $SmA_2 \rightarrow$ isotropic transitions; $T - T_{SmA_2-I} = 20$ °C in Figure 5. The intensities of the low-angle diffraction peaks decrease abruptly, broaden, and move to higher angles (i.e., shorter distances with greater dispersity) as the temperature is raised above $T_{SmA_2 \rightarrow I}$, but they do not disappear (Figure 5c). By optical microscopy, however, the salts are not birefringent in their isotropic phases. Small molecular aggregates with proximal ionic headgroups are probably present.[25]

The Case for SmA_2 Phases of nPmA (and nNmA) Salts and a Model for Their Packing. The SmA_2 assignment for **nPmA** (and **nNmA**) mesophases is based primarily on optical microscopy and X-ray diffraction data. The homeotropic textures require that the lamellar assemblies be uniaxial; they cannot tilt, as in a smectic C phase, for instance.[22] Also, focal-conic optical textures such as that in Figure 4d, a characteristic of smectic A phases,[22] are present in all of our liquid-crystalline salts. Second, XRD patterns in the liquid-crystalline temperature ranges contain a low-angle peak that is indicative of a layered phase. The calculated lamellar spacing is larger than the maximum extended length of one constituent molecule but less than the length of two molecules. Since optical microscopy data demonstrate that the molecular directors are orthogonal to their layer planes, any packing arrangement must involve interdigitation and/or chain bending that preserves cylindrical symmetry. The broadness of the high-angle diffraction peaks is inconsistent with smectic phases of the B, E, G, or H type with orthogonal directors *and* specific *intra*plane ordering.[26] Regardless, more than one molecule is needed to span a layer unit.

Table 4. Calculated Cross-Sectional Areas (A_H) of **1PnA** Headgroups

A	A_H (Å^2)	A	A_H (Å^2)
NO_3	62	BF_4	69
Br	63	ClO_4	70
I	66	PF_6	81

To accommodate the d values and SmA_2 packing, we invoke the model in Figure 6b in which cations are assumed to adopt tripodal geometries with conformationally labile chains (Figure 6a). If *all-transoid* and fully extended, chains make approximate angles (α) between each other and angles ϕ to the normal of the lamellar surface; the values of α and ϕ are related (eq 1). The actual angles and the true extension of l must be different from the idealized values due to gauche bends along the chains.

$$\langle\cos(\alpha)\rangle = 1 - \frac{3}{2}\langle\sin^2(\phi)\rangle \qquad (1)$$

When the angles are adjusted empirically to make $d = 2l\cos(\phi)$, the α are significantly less than 109.5°, the value if the long chains are extended to three corners of a tetrahedron. Because the degree of chain bending should not vary greatly among the salts, analyses employing the maximum calculated angles provide valid comparisons.

The magnitude of ϕ is also related to the cross-sectional area the chains project onto their "ionic plane". By tilting, chains can project a sum area, A_{3C}, approximately equal to that of their headgroup, A_H. The cross-sectional area per tilted chain is ca. $A_o/\cos(\phi)$,[27] where $A_o \cong 21.2$ Å^2 (using a simple square array of chains as a model) and $A_{3C} = 3A_o/\cos(\phi)$ (Table 3).

Packing of Headgroups for nPmA Salts. Assuming that the ionic centers are arranged as a mosaic in a plane, the sum of the effective radii of a **1Pm** or **1Nm** cationic center (r_c) *and* its associated anion constitute the A_H in Table 4. The headgroups of crystalline **18P18I**, **12N12Br**, and several related tetra-*n*-alkyl salts pack in this way.[5] Each r_c is estimated to be the sum of the P−C (1.80 Å)[28] and C−H (1.09 Å)[28] covalent bond distances plus the van der Waals radius of hydrogen (1.17 Å).[29] Thermochemical radii[30] have been used to calculate the cross-sectional areas of all the anions except PF_6^-. It is taken to be the sum of the P−F covalent bond distance (in tetraphenylphos-

(25) Kelker, H.; Hatz, R. *Handbook of Liquid Crystals*; Verlag Chemie: Weinheim, 1980; p 240

(26) Demus, D.; Goodby, J.; Gray, G. W.; Spiess, H.-W.; Vill, V. *Handbook of Liquid Crystals, Fundamentals*; Wiley-VCH: New York, 1998; Vol. 1, p 640.

(27) Weidemann, G.; Brezesinski, G.; Vollhardt, D.; Mohwald, H. *Langmuir* **1998**, *14*, 6485.

(28) Allen, F. H.; Kennard, O.; Watson, D. G.; Brammer, L.; Orpen, A. G.; Taylor, R. *J. Chem. Soc., Perkin Trans. 2* **1987**, *12*, S1.

(29) Bondi, A. *J. Phys. Chem.* **1964**, *68*, 441.

(30) Jenkins, H. D. B.; Thakur, K. P. *J. Chem. Educ.* **1979**, *56*, 576.

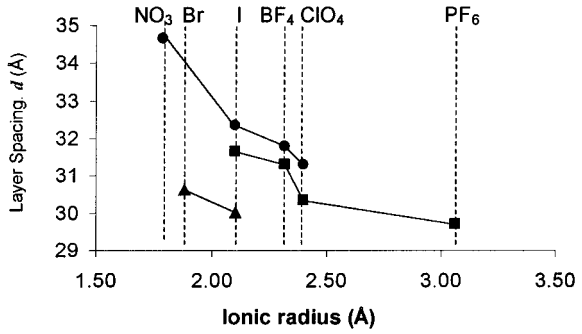

Figure 9. Dependence of **1P18A** SmA_2 layer spacing on the size of **A** at 80 °C (●), 90 °C (88 °C for **1P18PF$_6$**) (■), and 100 °C (▲).

phonium hexaflourophosphate;[31] 1.56 Å) and the van der Waals radius of fluoride[29] (1.50 Å). These A_H values underestimate the correct cross-sectional areas in the SmA_2 phases because larger lateral displacements caused by thermal motions are not included. They are incorporated into the A_{3C}.

The molecular arrangements within the SmA_2 phase suggest a direct relationship between *d* and **m**, the carbon chain length of the three equivalent *n*-alkyl groups. Although the *d* values for the three **1PmBF$_4$** salts (**m** = **10**, **14**, **18**) are from X-ray diffraction data recorded at different temperatures, they increase linearly with **m**: $d = 1.43\mathbf{m} + 6.17$ ($R^2 = 0.99$).

The values of *d* are also affected by larger **n** or **A**. Each increases A_H and necessitates more chain tilting ($>\phi$) within a lipophilic part of a lamella, leading to larger A_{3C} (Table 3). Thus, the spacings of the **1PmA** from measurements near a common temperature decrease as the anions[29−31] become larger (Figure 9). Although lengthening the short chain (i.e., >**n**) does not increase A_H directly, it does add volume constraints to regions immediately above and below the ionic plane. In our packing model, the **n** group is projected onto the opposite side of the ionic plane from its three long **m** chains. Greater length (or volume) of the **n** group is compensated by additional tilting of **m** chains.

Liquid-Crystal Phases of Group VA Salts with 1−4 Long *n*-Alkyl Chains. Is There a Common Theme? The magnitude and directionality of electrostatic interactions among ionic headgroups (responsible for overall phase anisotropy after "melting" of chains) is only one of several factors responsible for the nature of the ordering in phases of **nNmA**, **nPmA**, and related salts with *one, two*, or *four* long *n*-alkyl groups. For instance, electrostatic factors, alone, do not explain why tri-*n*-octadecylphophine oxide (with **P═O ↔ P$^+$—O$^-$** headgroups), some **nNmA** and **nPmA** salts, and *all* corresponding ammonium and phosphonium salts with *four* equivalent long *n*-alkyl chains examined thus far[5] are not liquid-crystalline. Segregation of the ionic and lipophilic regions and packing of the long chains are determined by several additional factors, including the following: (1) overall molecular shape; (2) the area of the ionic (head)-group (including the anion); (3) the type of shorter chain(s); and (4) the lengths and number of long *n*-alkyl chains. Because we now have information concerning Group VA salts with 1−4 long *n*-alkyl chains (and the remainder as short alkyl groups), their crystalline and liquid-crystalline phases will be compared briefly.

At elevated temperatures, crystalline ammonium salts with *one* long *n*-alkyl chain (i.e., interdigitated bilayers with *all-transoid* conformations and headgroups in rough planes[32]) become SmA_2 phases (Figure 10, $N = 1$).[1] Headgroups of crystalline ammonium bromide salts with *two* equivalent long *n*-alkyl groups are also in rough planes, but one of each pair of chains has two consecutive gauche bends near its cationic center (Figure 10, $N = 2$).[33] When heated above their melting temperatures, some of these (as well as the corresponding phosphonium) salts become SmA_2 phases[2a] with less interdigitation due to greater spatial constraints in the lipophilic regions. The molecular packing of SmA_2 phases of salts with two long *n*-alkyl groups and that of the **1PmA** (and **1NmA**) are markedly different (see Figure 2, Supporting Information).

Unfortunately, the crystal structure of only one Group VA salt with three long chains and a "simple" anion, **BzN18Br**, is known.[12] Although it may not be common to many other **nNmA** and **nPmA**, the crystal packing arrangement of **BzN18Br** is interesting as a comparison with the liquid-crystalline (SmA_2) bilayer arrangements in Figure 6b. Headgroups of crystalline **BzN18Br** form ionic planes that are less staggered than the charged centers of salts with one or two long alkyl chains. They separate alternating noninterdigitated and interdigitated layers comprised of respectively intramolecularly paired and intermolecularly paired (antiparallel) chains (Figure 10, $N = 3$).

The arrangement of the packing of headgroups of crystalline **BzN18Br** is somewhat like that of ammonium and phosphonium salts with *four* long alkyl chains.[5] At the supermolecular level, salts with four long *n*-alkyl chains stack in *monolayers* with a well-ordered "ionic plane" in the middle of each layer (Figure 10, $N = 4$). Two chains of each molecule are projected from one side of the ionic plane and two chains are projected from the other side. Depending on their length, chains may be either paired or projected away from each other in the lipophilic layers.[5]

In addition to the preferred packing arrangement for the liquid-crystalline phases of the **1PmA** shown in Figure 6 and in structure a of Figure 10 ($N = 3$), there are others that are consistent with the XRD and optical microscopy data. Two reasonable candidates are shown in Figure 10, structures b and c. They are somewhat analogous to the crystalline packing arrangements of $N = 4$ in that long alkyl chains of each molecule are projected on both sides of an ionic plane. Our preference for structure a is based primarily on the deleterious consequences that structures b and c would have on electrostatic interactions within ionic planes. In each, at least the α-methylene (or methyl) of the short alkyl group must lie approximately within an ionic layer. Its presence will disturb significantly the mosaic of alternating ionic charges from Y^+ and A^- that must be a major contributor to the stabilization of smectic motifs. These deleterious disruptions are not present in structure a and it allows the

(31) Banbery, H. J.; Hamor, T. A. *Acta Crystallogr.* **1988**, *C44*, 1683.

(32) Crystal structures. (a) *n*-decylammonium chloride: Pinto, A. V. A.; Vencato, I.; Gallardo, H. A.; Mascarenhas, Y. P. *Mol. Cryst. Liq. Cryst.* **1987**, *149*, 29. (b) *n*-dodecylammonium chloride: Silver, J.; Marsh, P. J.; Frampton, C. S. *Acta Crystallogr.* **1995**, *C51*, 2432. (c) *n*-Undecylammonium chloride monohydrate: Silver, J.; Martin, S.; Marsh, P. J.; Frampton, C. S. *Acta Crystallogr.* **1996**, *C52*, 1261. (d) *n*-Dodecylammonium bromide: Lunden, B. M. *Acta Crystallogr.* **1974**, *B30*, 1756. (e) *n*-Hexadecyltrimethylammonium bromide: Campanelli, A. R.; Scaramuzza, L. *Acta Crystallogr.* **1986**, *C42*, 1380. (f) *n*-Dodecyltrimethylammonium bromide: Kamitori, S.; Sumimoto, Y.; Vongbupnimit, K.; Noguchi, K.; Okuyama, K. *Mol. Cryst. Liq. Cryst.* **1997**, *300*, 31. (g) Benzyl-*n*-dodecyldimethylammonium bromide monohydrate: Rodier, N.; Dugue, J.; Ceolen, R.; Baziard-Mouysset, G.; Stigliani, J.-L.; Payard, M. *Acta Crystallogr.* **1995**, *C51*, 954.

(33) (a) Dimethyldi-*n*-tetradecylammonium bromide monohydrate: Okuyama, K.; Iijima, N.; Hirabayashi, K.; Kunitake, T.; Kusunoki, M. *Bull. Chem. Soc. Jpn.* **1988**, *61*, 2337. (b) Dimethyldi-*n*-octadecylammonium bromide: Kajiyama, T.; Kumano, A.; Takayanagi, M.; Kunitake, T. *Chem. Lett.* **1984**, 915. (c) Dimethyldi-*n*-octadecylammonium bromide monohydrate: Okuyama, K.; Soboi, Y.; Iijima, N.; Hirabayashi, K.; Kunitake, T.; Kajiyama, T. *Bull. Chem. Soc. Jpn.* **1988**, *61*, 1485.

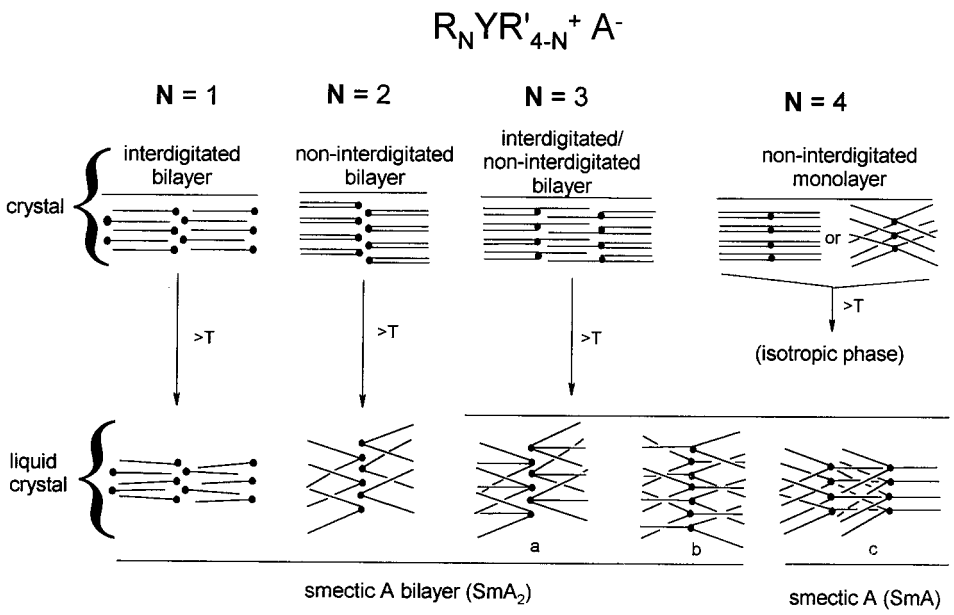

Figure 10. Cartoon representations of lamellar packing arrangements of Group VA salts with one to four long *n*-alkyl groups. R = $H(CH_2)_x$- where $x \geq 10$, R′ = $H(CH_2)_y$−, where $y \leq 4$ or benzyl, A = halide, and Y = nitrogen or phosphorus. Three of the possible packing arrangements are shown for the liquid-crystalline phase of salts when $N = 3$; "a" is the same representation as Figure 6b.

short chain to experience some attractive interactions by projecting it into a lipophilic region.

Thus, segregation of ionic groups in planes is retained in the crystalline and liquid-crystalline packing motifs of all of the Group VA salts. The assemblies are layered regardless of the number of long *n*-alkyl chains attached to the cationic center. The detailed nature of the packing and whether a liquid-crystalline phase can form depends primarily upon factors (2) and (3) above.

Conclusions

The phase behavior of the **nPmA** (and **nNmA**) salts examined here fills a gap in our knowledge of the relationship between amphiphile structure and packing within a neat phase.[8] In their mesophases, the phosphonium salts incorporate both order and mobility in segregated, alternating regions of high ionic and lipophilic character. Viewed as a set, the packing of Group VA salts with 1−4 long *n*-alkyl chains and simple anions follows a relatively clear pattern. As the cross-sectional areas of the chains of one molecule become increasingly larger than the area of their headgroup, the molecules balance the two by placing chains on opposite sides of the ubiquitous ionic planes. The progression is shown in cartoon form in Figure 10. The **nNmA** and **nPmA**, with *three* long *n*-alkyl chains, are pivotal: the sole example of their crystalline packing is like that of salts with *four* long chains, but their liquid-crystalline packing arrangements resemble those of salts with *two* long chains. To exhibit a SmA_2 phase, **nPmA** (and **nNmA**) salts require larger anions than the corresponding salts with *two* long *n*-alkyl chains. In this way, headgroups of the **nPmA** and their chains are able to project comparable cross-sectional areas onto the ionic planes. The next challenge will be to devise a theory like that for lyotropic phases[8] to explain the subtle, yet clear, packing differences among salts with 1−4 long *n*-alkyl chains and different headgroup areas!

The focus of this work has been on the characterization of the structures and properties of the anisotropic phases of **nPmA** (and **nNmA**) salts. However, there are many potential applications that we hope to explore in the future. For instance, related isotropic ionic fluids have received considerable attention as "green solvents" because they are nonvolatile and can be recycled.[9a] The incorporation of order within ionic fluids,[9b,c] as accomplished here, may allow the **nPmA** to exert additional control over reactions of their solutes.[10] Also, because liquid-crystalline **nPmA** salts are completely saturated, they should be useful in spectroscopic studies and reactions where conditions preclude the use of media with unsaturated groups such as those in ionic liquids based on imidazolium.[9b,c,34] Preliminary studies have shown that thermotropic and lyotropic liquid-crystalline phases of the corresponding ammonium salts have potential uses in NMR structural studies[35] (like those by Bax et al. in aqueous lyotropic liquid crystals[36]). We expect that the phosphonium salts will be even more versatile for such purposes due to their greater thermal stabilities and wider liquid-crystalline temperature ranges.

Acknowledgment. The National Science Foundation is gratefully acknowledged for its support of this research. The authors thank Prof. Frank Quina of the Universidade de São Paulo for informing us of the method of Supulveda for anion exchanges[14] and Prof. Timothy Swager of the Massachusetts Institute of Technology for use of his powder diffractometer.

Supporting Information Available: Two additional tables summarizing the DSC data for **nP18Br** and **nP18I**, preparative procedures and physical and spectroscopic data for salts used in this study, a discussion of the relationship between the salts presented here and similar salts with two long *n*-alkyl chains (including one figure), and a figure showing the XRD patterns of **1P18I** and **1N18I** (PDF). This material is available free of charge via the Internet at http://pubs.acs.org.

JA994055G

(34) (a) Earle, M. J.; McCormac, P. B.; Seddon, K. R. *J. Chem. Soc., Chem. Commun.* **1998**, *20*, 2245. (b) Hondrogiannis, G.; Lee, C. W.; Pagni, R. M.; Mamantov, G. *J. Am. Chem. Soc.* **1993**, *115*, 9828.

(35) Lu, L.; Nagana Gowda, G. A.; Suryaprakash, N.; Khetrapal, C. L.; Weiss, R. G. *Liq. Cryst.* **1998**, *25*, 295.

(36) See for instance: Ramirez, B. E.; Bax, A. *J. Am. Chem. Soc.* **1998**, *120*, 9106.